Mater. Res. Soc. Symp. Proc. Vol. 892 © 2006 Materials Research Society 0892-FF11-02.1

The mean inner potential of GaN measured from nanowires using off-axis electron holography

Andrew S. W. Wong[1], Ghim W. Ho[2], Rafal Dunin-Borkowski[1,3], Takeshi Kasama[3,1], Rachel A. Oliver[1], Pedro M.F.J. Costa[1] and Colin. J. Humphreys[1]

[1]Department of Materials Science and Metallurgy, University of Cambridge, Pembroke Street, Cambridge CB2 3QZ, United Kingdom.
[2] Nanoscience Centre, University of Cambridge, 11 JJ Thomson Avenue, Cambridge CB3 0FF, United Kingdom.
3 Frontier Research System, The Institute of Physical and Chemical Research, Hatoyama, Saitama 350-0395, Japan.

ABSTRACT

The mean inner potentials of wurtzite GaN nanowires are measured using off-axis electron holography in the transmission electron microscope (TEM). The nanowires have a circular cross-section and are suspended across holes in a holey carbon film, resulting in an accurate knowledge of their thickness profiles and orientations. They are also free of the implantation and damage that is present in mechanically-polished ion-milled TEM specimens. The effect of a thin amorphous coating, which is present on the surfaces of the nanowires, on measurements of their mean inner potential is assessed. A value for the mean inner potential of GaN of (16.7± 0.3) V is obtained from these samples.

INTRODUCTION

The technique of off-axis electron holography in the transmission electron microscope (TEM), which is described in detail elsewhere [1-3] allows the phase shift ϕ of a high-energy electron that has passed through a specimen to be measured. In the absence of magnetic fields, the phase shift is, in turn, directly proportional to the electrostatic potential in the specimen V integrated in the electron beam direction, according to the equation

$$\phi(x,y) = C_E \int_{-\infty}^{\infty} V(x,y,z)dz \quad (1)$$

where C_E takes a value of 6.53×10^6 rad $V^{-1}m^{-1}$ at a microscope accelerating voltage of 300 kV. If V is constant throughout specimen thickness t, then Eq. 1 can be expressed more simply in the form

$$\phi(x,y) = C_E V(x,y)\, t(x,y) \quad (2)$$

A major contribution to V is associated with the mean inner potential V_o. When using off-axis electron holography to quantify piezoelectric fields in InGaN/GaN quantum wells [4-5] an accurate knowledge of V_o is desirable. In most materials, V_o takes a value between 5 and 30V [3], depending on the composition and structure of the material. Its value is highly sensitive to variations in charge density associated with bonding and ionicity. Traditionally, experimental values of V_o in many

semiconductors have been measured using wedge-shaped cleaved specimens [6-7], which are relatively free of the surface damage that is associated with preparing TEM specimens using ion milling. If the wedge angle is known, then according to Eq. 2 the specimen thickness profile can be correlated precisely with a phase profile measured using electron holography in order to determine V_o. Unfortunately, measurement of V_o for GaN typically suffers from the difficulty of cleaving wedges of epitaxial layers of GaN that have been grown on sapphire or silicon carbide. Accordingly, here we examine crystalline nanowires of GaN, which have a known thickness profile, to measure V_o in GaN. Errors resulting from the effect of dynamical diffraction on the measured phase shift are reduced by ensuring kinematical diffraction conditions [3], while the presence of electrostatic fields due to charging of the sample [7-8] is discounted by checking that the phase gradient on either side of each GaN nanowire examined is identical.

EXPERIMENTAL DETAILS

Crystalline GaN nanowires were synthesized in a chemical vapor deposition reactor using a Ni catalyst. Nanowire growth was carried out on SiO_2/Si substrates that were held at 1050°C for 30 minutes. Metallic Ga was used as the group III source, while ammonia was used as the group V source. The nanowires had diameters of between 5 and 20 nm. Nanowires of diameter ~13 nm were selected for electron holography as a compromise between poor statistics obtained from narrower nanowires and increased likelihood of faceting in larger diameter nanowires. Electron energy-loss spectroscopy (not presented here) was used to confirm that the nanowires comprised Ga and N.

The GaN nanowires were transferred onto a holey carbon copper grid by placing the carbon film on the substrate surface. Organic solvents such as ethanol were avoided in order to reduce contamination of the nanowires. Off-axis electron holography was carried out using a Philips CM300-ST field emission gun TEM equipped with a Möllenstedt-Düker biprism. Holograms were acquired using a 2048 pixel charged-couple-device camera and a biprism voltage of 160 V. The field of view in each hologram was 40 nm, with 8 pixels/holographic fringe and a fringe contrast of 30 %. The magnification was calibrated accurately using graphitized carbon. Reference holograms acquired from vacuum were used to remove distortions associated with the imaging and recording systems of the microscope.

EXPERIMENTAL RESULTS AND DISCUSSION

A scanning electron micrograph of a region of nanowires dispersed on the holey carbon film is shown in Fig. 1. In the TEM, nanowires that were suspended across holes were chosen for examination using electron holography and tilted away from strongly diffracting orientations.

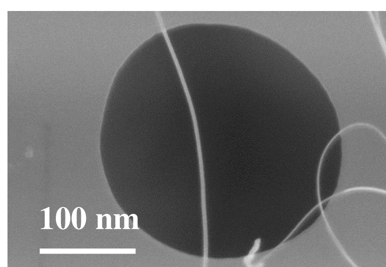

Figure 1: Scanning electron micrograph showing nanowires dispersed on a TEM grid. The grey region is the carbon film while the dark region is a hole in the film.

Figures 2a and b show representative phase and amplitude images, respectively, acquired from a single nanowire using electron holography. Line profiles (averaged over a distance of 1.5 nm) were extracted from each phase image in a direction perpendicular to the longitudinal axis of the nanowire. Simulations based on Eqs. 1 and 2 were then fitted to each experimental profile using two models for the cross-sectional form of the nanowire, which are illustrated schematically in Fig. 3. Model 1 assumed the nanowire to have a circular cross-section and a uniform composition. Model 2, which attempts to account for the presence of a thin amorphous layer visible around each nanowire, assumed the nanowire to have a core of circular cross-section surrounded by a thin shell of different material. For Model 1, the mean inner potential and diameter of the nanowire were fitted. For Model 2, the mean inner potential and the thickness of the shell were also included in the fit.

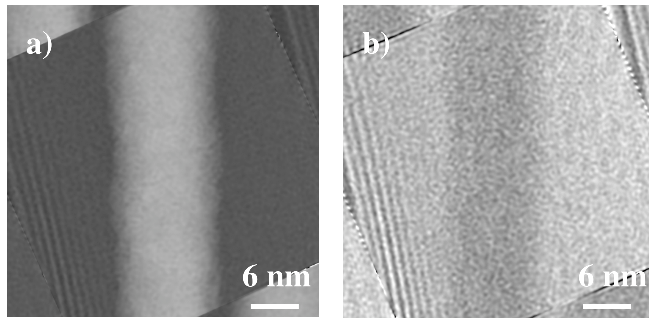

Figure 2: (a) Phase and (b) amplitude images measured from a single nanowire. The image size is 512 x 512 pixels.

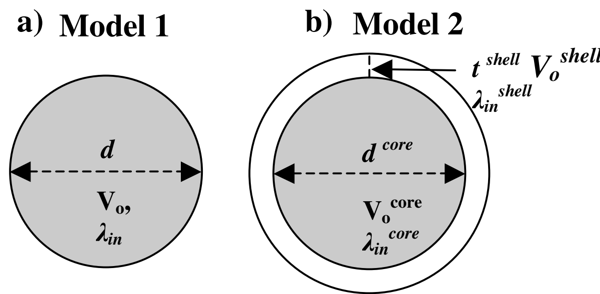

Figure 3: Schematic diagrams showing the cross-section of a nanowire for (a) Model 1 and (b) Model 2. V_o, d, t and λ_{in} denote mean inner potential, diameter, thickness and inelastic mean free path, respectively.

Figures 4a and b show best-fitting simulated phase profiles to an experimental phase profile, obtained using Models 1 and 2, respectively. Model 2 consistently provided the better match to the experimental profiles, which were always consistent with the expected circular cross-section of each nanowire.

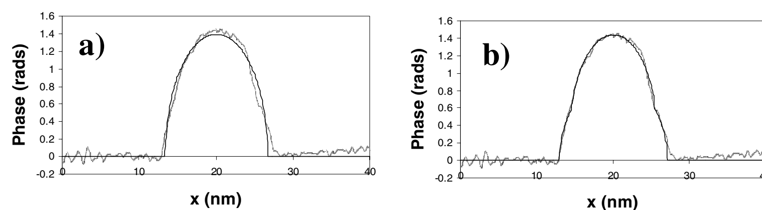

Figure 4: Experimental phase profiles obtained from selected region in Figure 2a. The fitted profiles using (a) Model 1 and (b) Model 2 are displayed along with the experimental profiles. Experimental and fitted profiles are dashed and solid lines, respectively.

Figures 5a and b show histograms of the fitted values of nanowire mean inner potential and diameter, respectively, obtained by applying Model 1 to 40 experimental

phase profiles acquired from 15 different nanowires. Figures 6a and b shows fitted values for the mean inner potential and diameter, respectively, for the core of the wire obtained using Model 2. Figures 6c and d show corresponding fitted values for the mean inner potential and the thickness of the shell around each nanowire. The measurements shown in Figs. 5 and 6 are summarized in Table 1.

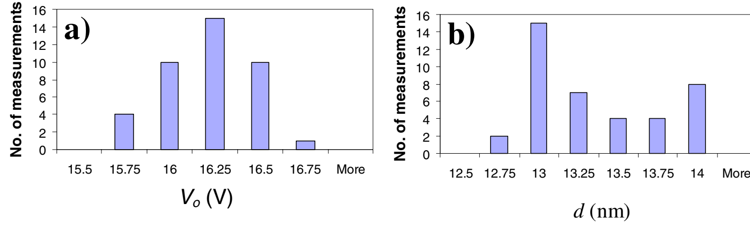

Figure 5: Histograms of (a) V_o and (b) d obtained by fitting experimental phase profiles using Model 1.

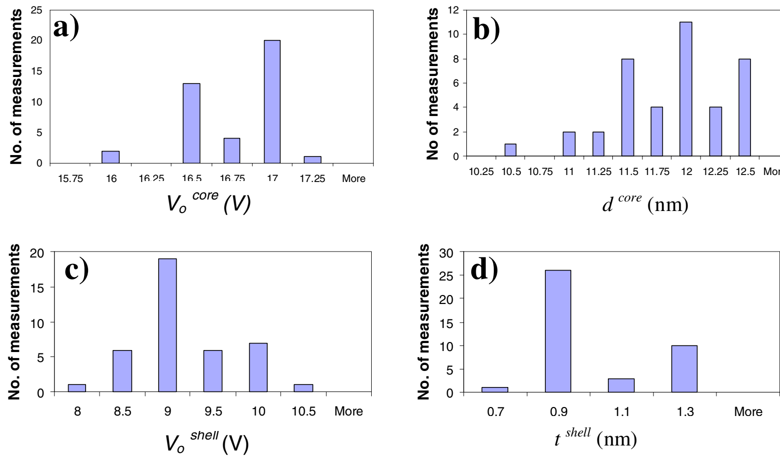

Figure 6: Histograms of (a) V_o^{core} and (b) d^{core}, (c) V_o^{shell} and (d) t^{shell}, obtained by fitting experimental phase profiles using Model 2.

Table 1: Parameters fitted to experimental phase profiles.

	Model 1		Model 2			
	V_o (V)	d (nm)	V_o^{core} (V)	d^{core} (nm)	V_o^{shell} (V)	t^{shell} (nm)
Mean	16.12	13.24	16.67	11.78	9.01	0.94
Standard deviation	0.24	0.42	0.27	0.50	0.57	0.19
Standard error in the mean	0.037	0.066	0.042	0.080	0.090	0.030

Figures 7a and b additionally show the fitted mean inner potential of the nanowire, obtained using Model 1s and 2, respectively, plotted as a function of the parameter

$$V_o \lambda_{in} = \frac{\phi}{-2C_E \ln A} \quad (3)$$

measured at the centre of the nanowire, where λ_{in} is the inelastic mean free path and A is the normalized amplitude of the reconstructed image wave (Fig. 2b). This plot allows the effect of dynamical diffraction on the phase images to be monitored, since λ_{in} is expected to be influenced by diffraction contrast. There is little scatter in the data points shown in Fig. 7, suggesting that kinematical diffracting conditions have been achieved successfully for the experimental measurements.

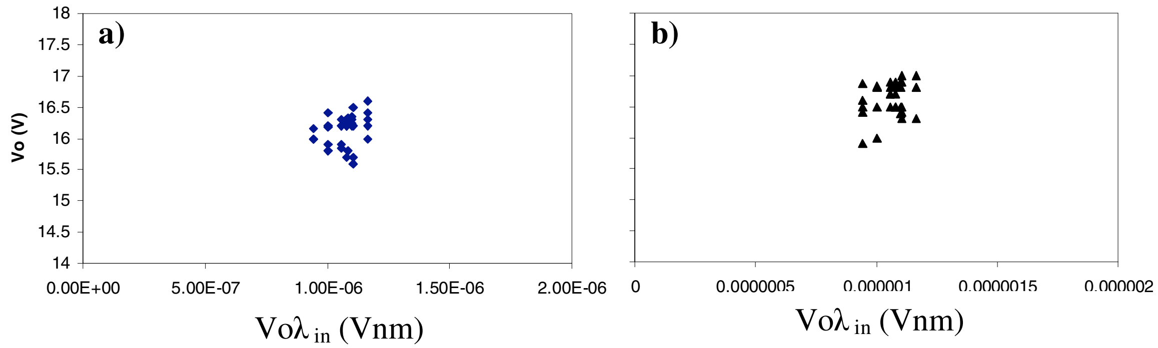

Figure 7: Fitted values of V_o plotted as a function of $V_o\lambda_{in}$ for (a) Model 1 and (b) Model 2.

Two aspects of the measurements shown in Figure 5-7 are significant. First, if amorphous shell around the nanowires, which has a mean thickness only of 0.94 nm, is not considered then the fitted mean inner potential of the nanowires is altered by 0.55 V on average. Although its nature has not been established experimentally, the fitted mean inner potential of the shell is consistent with that expected for amorphous carbon. Second, the best-fitting value for V_o of the GaN core obtained using Model 2, of (16.7 ±0.3) V, is significantly different from reported in literature [9].

Reassuringly, our value is close to that expected on the basis of lower and upper bounds for values of V_o calculated using the scattering factors of Radi [3] and Doyle and Turner [3].

On a final note, it should be remembered that specimens can charge under the illumination of the electron beam [7, 8]. Evidence for the presence of charging of a nanowire during TEM examination is shown in the form of experimental phase contours (Fig. 8a) and a phase profile extracted across the nanowire (Fig. 8b).

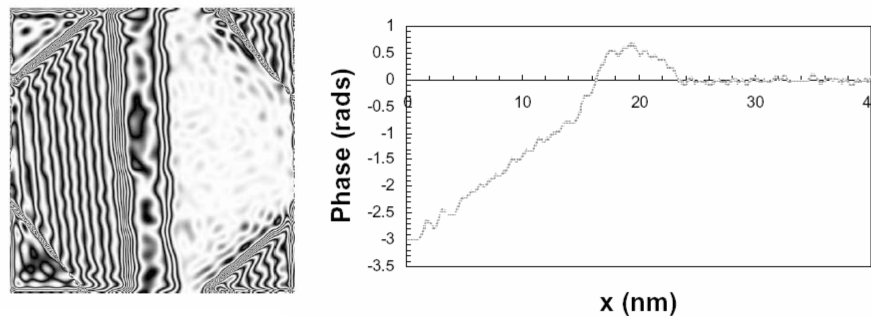

Figure 8: (a) 32 times amplified phase image of a charging nanowire. (b) Phase profile across the nanowire. The slope in the phase of the vacuum on the left indicates that the nanowire is charged.

Charging results in a different phase gradient in vacuum on each side of the nanowire, indicating that it is unsuitable for measurement of its mean inner potential.

CONCLUSIONS

15 different GaN nanowires of average diameter 13 nm have been characterised using off-axis electron holography. A value for the mean inner potential of GaN of (16.67 ± 0.3) V has been measured from these samples.

ACKNOWLEDGEMENTS

ASW and GWH acknowledge the Cambridge Commonwealth Trust. RDB, RAO and PMDFC also acknowledge the the Royal Society, the Royal Commission for the Exhibition of 1851 and the Engineering and Physical Sciences Research Council (EPSRC) for financial support, respectively.

REFERENCES

1. R.E. Dunin-Borkowski, M.R. McCartney, D.J. Smith, *Electron holography of nanostructured materials* in: H.S. Nalwa (Ed.), Encyclopaedia of Nanoscience and Nanotechnology, Vol 3, American Scientific Publishers, Stevenson Ranch, CA, (2004).
2. A. Tonomura, L.F. Allard, G. Pozzi, D.C. Joy and Y.A. Ono (Eds.), *Electron holography*, Elsevier, Amsterdam, (1995).
3. E. Völkl, L.F. Allard and D.C. Joy (Eds.), *Introduction to Electron Holography*, Plenum, New York, (1998).
4. M. Takeguchi, M.R. McCartney and D.J. Smith, *Appl. Phys. Lett.* 84, 2103 (2004).
10. M. Stevens, A. Bell, M.R. McCartney, F.A. Ponce, H. Marui and S. Tanaka, *Appl. Phys. Lett.* 85, 4651 (2004).
5. J. Li, M.R. McCartney, R.E.Dunin-Borkowshi, and D.J. Smith, *Acta Cryst*. A 55, 652 (1999).
6. M. Gajdardziska-Josifovska, M.R. McCartney, W.J. de Ruijter, D.J, Smith, J.K. Weiss and J.M. Zuo, Ultramicroscopy 50, 285 (1993).
7. M.R. McCartney, M.A. Gribelyuk, J. Li, P. Rosheim, J.S. McMurray and D.J. Smith, *Appl. Phys. Lett.* 80, 3213 (2002).
8. R.E. Dunin-Borkowski, S.B. Newcomb, T. Kasama, M.R. McCartney, M. Weyland and P.A. Midgley, *Ultamicroscopy* 103, 67 (2005).
9. J.S. Barnard, M.J. Kappers, E.J. Thrush and C.J. Humphreys, in *Microscopy of Semiconducting Materials 2003*, Inst. of Physics, Bristol and Philadelphia, 281 (2003).